Photophysics of π-Conjugated Metal−Organic Oligomers: Aryleneethynylenes that Contain the (bpy)Re(CO)$_3$Cl Chromophore

Keith A. Walters,[†] Kevin D. Ley,[†] Carla S. P. Cavalaheiro,[†] Scott E. Miller,[§] David Gosztola,[||] Michael R. Wasielewski,[§] Alejandro P. Bussandri,[‡] Hans van Willigen,[‡] and Kirk S. Schanze*,[†]

Contribution from the Department of Chemistry, University of Florida, PO Box 117200, Gainesville, Florida 32611-7200, Division of Chemistry, Argonne National Laboratory, Argonne, Illinois 60439, Department of Chemistry, Northwestern University, 2145 Sheridan Road, Evanston, Illinois 60208, and Department of Chemistry, University of Massachusetts, Boston, Massachusetts 02125

Received March 13, 2001. Revised Manuscript Received June 23, 2001

Abstract: A comprehensive study of a series of four monodisperse, metal−organic π-conjugated oligomers of varying length is reported. The oligomers are based on the aryleneethynylene architecture, and they contain a 2,2′-bipyridine-5,5′-diyl (bpy) metal binding unit. The photophysical properties of the free oligomers and their complexes with the (L)Re^{I}(CO)$_3$X chromophore (where L = the bpy-oligomer and X = Cl or NCCH$_3$) were explored by a variety of methods including electrochemistry, UV−visible absorption, variable temperature photoluminescence (PL), transient absorption (TA), and time-resolved electron paramagnetic spectroscopy (TREPR). The absorption of the free oligomers and the metal complexes is dominated by the π,π^* transitions of the π-conjugated oligomers. The free oligomers feature a strong blue fluorescence that is quenched entirely in the (L)Re^{I}(CO)$_3$X complexes. The metal−oligomers feature a weak, relatively long-lived red photoluminescence that is assigned to emission from both the $^3\pi,\pi^*$ manifold of the π-conjugated system and the dπ Re $\rightarrow \pi^*$ bpy-oligomer metal-to-ligand charge transfer (^{3}MLCT) state. On the basis of a detailed analysis of the PL, TA, and TREPR results an excited-state model is developed which indicates that the oligomer-based $^3\pi,\pi^*$ state and the ^{3}MLCT states are in close energetic proximity. Consequently the photophysical properties reflect a composite of the properties of the two excited-state manifolds.

Introduction

π-Conjugated polymers and oligomers have been the focus of considerable research during the past 2 decades. Much of the work on π-conjugated materials has focused on exploring the chemical and physical basis for their unique electronic and optical properties.[1,2] However, there also is a significant possibility that π-conjugated materials may comprise the basis for a new generation of organic material-based electronic and photonic devices.[3,4]

Studies of organic π-conjugated materials have explored the relationship between molecular structure and the properties of the materials. Properties of interest include the band-gap and absorption spectra,[5] thermal- and photoconductivity,[6−8] photo- and electroluminescence,[9,10] electrochromism,[11] and nonlinear optical response.[12] This work has led to the development of a reasonably clear picture of how molecular-level structure influences the optical and electronic properties of a material. Although much of the work in this area has focused on medium- to high-molecular weight polymers, many investigations have explored the optical and electronic properties of low- to medium-molecular weight monodisperse oligomers.[13−27] The oligomer

* To whom correspondence should be addressed, kschanze@chem.ufl.edu.
[†] University of Florida.
[§] Northwestern University.
[||] Argonne National Laboratory.
[‡] University of Massachusetts.

(1) *Advances in Synthetic Metals. Twenty Years of Progress in Science and Technology*; Bernier, P., Lefrant, S., Bidan, G., Eds.; Elsevier Science SA: Amsterdam, 1999.
(2) *Handbook of Conducting Polymers*, 2nd ed.; Skotheim, T. A., Elsenbaumer, R. L., Reynolds, J. R., Eds.; Marcel Dekker: New York, 1998.
(3) Kraft, A.; Grimsdale, A. C.; Holmes, A. B. *Angew. Chem., Int. Ed.* **1998**, *37*, 402−428.
(4) For a recent compilation of papers that discuss fundamentals and applications of π-conjugated materials see: *Acc. Chem. Res.* **1999**, *32*, issue 3.
(5) Patil, A. O.; Heeger, A. J.; Wudl, F. *Chem. Rev.* **1988**, *88*, 183−200.
(6) Lee, C. H.; Yu, G.; Pakbaz, K.; Moses, D.; Sariciftci, N. S.; Wudl, F.; Heeger, A. J. *Synth. Met.* **1995**, *70*, 1353−1356.
(7) Lee, C. H.; Yu, G.; Moses, D.; Pakbaz, K.; Zhang, C.; Sariciftci, N. S.; Heeger, A. J.; Wudl, F. *Phys. Rev. B* **1993**, *48*, 15425−15433.
(8) Barth, S.; Bassler, H. *Phys. Rev. Lett.* **1997**, *79*, 4445−4448.
(9) Burroughes, J. H.; Bradley, D. D. C.; Brown, A. R.; Marks, R. W.; Mackay, K.; Friend, R. H.; Burn, P. L.; Holmes, A. B. *Nature* **1990**, *347*, 539−541.
(10) Bassler, H.; Rothberg, L. J. *Chem. Phys.* **1998**, *227*, 1−270.
(11) Schwendeman, I.; Hwang, J.; Welsh, D. M.; Tanner, D. B.; Reynolds, J. R. *Adv. Mater.* **2001**, *13*, 634−637.
(12) Bredas, J. L.; Silbey, R. *Conjugated Polymers: The Novel Science and Technology of Highly Conducting and Nonlinear Optically Active Materials*; Kluwer: Boston, 1991.
(13) Becker, R. S.; de Melo, J. S.; Maçanita, A.; Elisei, F. *J. Phys. Chem.* **1996**, *100*, 18683−18695.
(14) de Melo, J. S.; Silva, L. M.; Arnaut, L. G.; Becker, R. S. *J. Chem. Phys.* **1999**, *111*, 5427−5433.
(15) Cornil, J.; dos Santos, D. A.; Beljonne, D.; Bredas, J. L. *J. Phys. Chem.* **1995**, *99*, 5604−5611.
(16) Mullen, K.; Wegner, G. *Adv. Mater.* **1998**, *10*, 433−436.
(17) Moroni, M.; Moigne, J. L.; Luzzati, S. *Macromolecules* **1994**, *27*, 562−571.
(18) Wautelet, P.; Moroni, M.; Oswald, L.; Moigne, J. L.; Pham, A.; Bigot, J.-Y. *Macromolecules* **1996**, *29*, 446−455.
(19) Young, J. K.; Moore, J. S. In *Modern Acetylene Chemistry*; Diederich, F., Stang, P. J., Eds.; VCH: Weinheim, 1995; pp Chapter 12.
(20) Moore, J. S. *Acc. Chem. Res.* **1997**, *30*, 402−413.

10.1021/ja015813h CCC: $20.00
Published on Web 08/04/2001

work is very important, since it allows scientists to understand the important relationship between conjugation length and electronic and optical properties of the materials.[16,24]

More recently, a number of groups have examined the optical and electronic (or electrochemical) properties of π-conjugated materials that contain transition metals that interact strongly with the delocalized π-electron systems.[28−47] These efforts have the objective of using the widely variable optical, electronic and magnetic properties of the metals as a tool to allow the design of π-conjugated polymers having unique materials properties. Although a number of advances have been made in this area, the complex electronic structure of transition-metal complexes hinders the detailed study of the effect of the metal on the delocalized π-electron system. Consequently, the need has arisen to examine well-defined oligomer model systems to provide a basis for understanding the interactions between the π-electron system and a transition-metal center.

One area that has received particular attention recently has been the study of poly(phenylenevinylene) (PPV)- and poly(phenyleneethynylene) (PPE)-type polymers that are "doped" with transition-metal bipyridine chromophores along the π-conjugated backbone.[28−41,45−48] These polymers are of interest because of the possibility that the transition metals will strongly influence the optical and electronic properties of the materials through the introduction of new accessible redox states and charge-transfer based excitations. Indeed, recent studies by Yu and co-workers,[34−36] and others[28−33,37−39,41,48] demonstrated that introduction of Ru(II)-, Os(II)- or Re(I)-bipyridine chromophores into the backbone of a PPV or PPE π-conjugated polymer has a dramatic influence on the absorption, photoluminescence (PL), photoconductivity, and photorefractivity of the materials. Although these studies demonstrate that the metals strongly influence the properties of the π-systems, due to the structural complexity of the polymers it is difficult to obtain detailed insight concerning the mechanisms by which the π-conjugated systems are modified by the presence of the transition-metal centers.

In view of the lack of detailed information concerning structure−property relationships for π-conjugated metal−organic systems, we initiated a study having the objective of synthesis and photophysical characterization of a series of structurally well-defined, high-molecular weight π-conjugated oligomers that contain the 2,2′-bipyridine unit as a metal binding site.[31] We selected as targets a series of oligomeric aryleneethynylenes (OAEs) that contain a 2,2′-bipyridine-5,5′-diyl metal chelating unit at their core. The choice of the OAE system was based on several factors including synthetic accessibility[31] and the expectation that the $^3\pi,\pi^*$ manifold in the OAEs would be comparatively high in energy, thereby minimizing complications that would arise due to interaction of the triplet states with metal complex-based charge-transfer states.

The present contribution provides a detailed report of the photophysical properties of unmetalated OAEs **1**−**4** (Scheme 1) and the metal−OAE complexes wherein $-Re^{I}(CO)_3X$ is coordinated to the 2,2′-bipyridine-5,5′-diyl moiety (X = Cl or CH_3CN, complexes **Re-1**−**Re-4** and **ReACN-2** and **ReACN-3**, Scheme 1). The (diimine)$Re^{I}(CO)_3X$ chromophore was selected for these studies for several reasons: (1) Small molecule complexes of this type have been the focus of many photophysical investigations, and consequently the properties of this chromophore are well understood.[49−51] (2) (Diimine)$Re^{I}(CO)_3X$ complexes feature a lowest excited-state based on dπ Re $\rightarrow$ π^* diimine metal-to-ligand charge transfer (MLCT), and the energy of this state can be predicted based on the reduction potential of the diimine acceptor ligand.[50,51] The MLCT excited state is typically long-lived and photoluminescent and gives rise to a strong and characteristic transient absorption in the near-UV and visible.[50,51] These features make it relatively easy to detect and characterize the Re $\rightarrow$ diimine MLCT state even in complex supramolecular systems.

Experimental Section

Synthesis and Characterization of 1−4 and Re-1−Re-4. The methodology used to synthesize oligomers **1**−**4** relied extensively upon Sonogashira coupling of appropriately protected and functionalized aryl iodides and terminal acetylenes.[52] Details of the synthesis and complete characterization of **1**−**4** and **Re-1**−**Re-4** are presented elsewhere.[31]

Synthesis of ReACN-2 and ReACN-3. The preparation involved Ag^+OTf^- promoted substitution of Cl for CH_3CN. The same procedure was followed for both complexes, and we provide the details for **ReACN-2**. **Re-2** (12 mg, 6.1 μmol) was dissolved in 20 mL of methylene chloride, whereupon 5 mL of CH_3CN and $Ag(CF_3SO_3)$ (12 mg, excess) was added. The solution was stirred at room temperature overnight. TLC of the reaction mixture (silica, 1:1 hexanes:CH_2Cl_2)

(21) Tour, J. M. *Chem. Rev.* **1996**, *96*, 537−553.
(22) Jones, L., II; Schumm, J. S.; Tour, J. M. *J. Org. Chem.* **1997**, *62*, 1388−1410.
(23) Huang, S. L.; Tour, J. M. *J. Org. Chem.* **1999**, *64*, 8898−8906.
(24) Martin, R. E.; Diederich, F. *Angew. Chem., Int. Ed.* **1999**, *38*, 1351−1377.
(25) Ziener, U.; Godt, A. *J. Org. Chem.* **1997**, *62*, 6137−6143.
(26) Kukula, H.; Veit, S.; Godt, A. *Eur. J. Org. Chem.* **1999**, *277*, 7−286.
(27) Remmers, M.; Müller, B.; Martin, K.; Räder, H.-J.; Köhler, W. *Macromolecules* **1999**, *32*, 1073−1079.
(28) Kingsborough, R. P.; Swager, T. M. *Prog. Inorg. Chem.* **1999**, *48*, 123−231.
(29) Ley, K. D.; Whittle, C. E.; Bartberger, M. D.; Schanze, K. S. *J. Am. Chem. Soc.* **1997**, *119*, 3423−3424.
(30) Ley, K. D.; Schanze, K. S. *Coord. Chem. Rev.* **1998**, *171*, 287−307.
(31) Ley, K. D.; Li, Y. T.; Johnson, J. V.; Powell, D. H.; Schanze, K. S. *Chem. Commun.* **1999**, 1749−1750.
(32) Ley, K. D.; Walters, K. A.; Schanze, K. S. *Synth. Met.* **1999**, *102*, 1585−1586.
(33) Walters, K. A.; Trouillet, L.; Guillerez, S.; Schanze, K. S. *Inorg. Chem.* **2000**, *39*, 5496−5509.
(34) Peng, Z.; Yu, L. *J. Am. Chem. Soc.* **1996**, *118*, 3777−3778.
(35) Peng, Z.; Gharavi, A. R.; Yu, L. *J. Am. Chem. Soc.* **1997**, *119*, 4622.
(36) Wang, Q.; Yu, L. *J. Am. Chem. Soc.* **2000**, *122*, 11806−11811.
(37) Zhu, S. S.; Swager, T. M. *J. Am. Chem. Soc.* **1997**, *119*, 12568−12577.
(38) Zhu, S. S.; Kingsborough, R. P.; Swager, T. M. *J. Mater. Chem.* **1999**, *9*, 2123-2131.
(39) Ng, W. Y.; Chan, W. K. *Adv. Mater.* **1997**, *9*, 716−719.
(40) Ng, P. K.; Gong, X.; Wong, W. T.; Chan, W. K. *Macromol. Rapid Commun.* **1997**, *18*, 1009−1016.
(41) Chan, W. K.; Ng, P. K.; Gong, X.; Hou, S. *J. Mater. Chem.* **1999**, *9*, 2103-2108.
(42) Harriman, A.; Ziessel, R. *J. Chem. Soc., Chem. Commun.* **1996**, 1707−1716.
(43) Harriman, A.; Khatyr, A.; Ziessel, R.; Benniston, A. C. *Angew. Chem., Int. Ed.* **2000**, *39*, 4287−4290.
(44) Schlicke, B.; Belser, P.; De Cola, L.; Sabbioni, E.; Balzani, V. *J. Am. Chem. Soc.* **1999**, *121*, 4207−4214.
(45) Wang, B.; Wasielewski, M. R. *J. Am. Chem. Soc.* **1997**, *119*, 12−21.
(46) Chen, L. X.; Jäger, W. J. H.; Niemczyk, M. P.; Wasielewski, M. R. *J. Phys. Chem. A* **1999**, *103*, 4341−4351.
(47) Chen, L. X.; Jäger, W. J. H.; Gosztola, D. J.; Niemczyk, M. P.; Wasielewski, M. R. *J. Phys. Chem. B* **2000**, *104*, 1950−1960.
(48) Rasmussen, S. C.; Thompson, D. W.; Singh, V.; Peterson, J. D. *Inorg. Chem.* **1996**, *35*, 3449−3450.
(49) Wrighton, M.; Morse, D. L. *J. Am. Chem. Soc.* **1974**, *96*, 998−1003.
(50) Worl, L. A.; Duesing, R.; Chen, P.; Della Ciana, L.; Meyer, T. J. *J. Chem. Soc., Dalton Trans.* **1991**, 849−858.
(51) Schanze, K. S.; MacQueen, D. B.; Perkins, T. A.; Cabana, L. A. *Coord. Chem. Rev.* **1993**, *122*, 63−89.
(52) Sonogashira, K. In *Comprehensive Organic Synthesis*; Trost, B. M.,-Fleming, I., Eds.; Pergammon Press: Oxford, 1991; Vol. 3, p 521.

Scheme 1

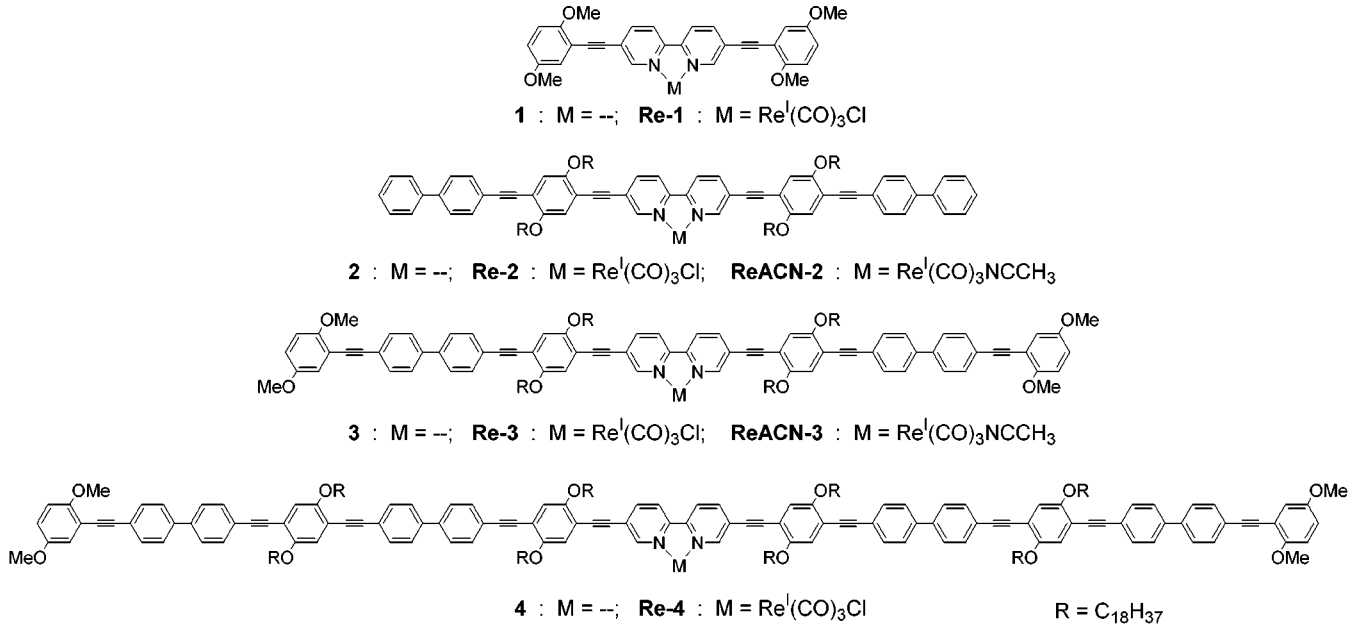

showed two spots, $R_f = 1$ (**ReACN-2**) and $R_f = 0.6$ (**Re-2**). Stirring for an additional 6 h allowed the reaction to go to completion. Solid AgCl was removed from the sample solution by filtration through Celite on a medium-porosity glass frit, and the solvent was removed under reduced pressure to afford **ReACN-2** as the $CF_3SO_3^-$ salt. Due to the small amount of material available, further purification was impractical.

Characterization of ReACN-2: IR (THF soln, cm^{-1}), 1966, 2101, 2135 ($\upsilon_{C\equiv O}$), 2278 ($\upsilon_{C\equiv N}$).[53] ESI-MS calcd for $C_{131}H_{182}N_3O_7Re$: 2096; found: 2053 (parent − CH_3CN).

Characterization of ReACN-3: IR (THF soln, cm^{-1}) 1967, 2097, 2133 ($\upsilon_{C\equiv O}$), 2280 ($\upsilon_{C\equiv N}$).[53] ESI-MS calcd for $C_{149}H_{195}N_2O_{11}Re$: 2416; found: 2414 (parent), 2372 (parent − CH_3CN).

Photophysical Measurements. All photophysical studies were conducted in 1 cm square quartz cuvettes unless otherwise noted. All room-temperature studies were conducted on THF solutions that were deoxygenated using argon bubbling, and all low-temperature studies were conducted on 2-methyltetrahydrofuran (2-MTHF) solvent glasses degassed by 4 freeze−pump−thaw cycles (ca. 10^{-4} Torr) unless otherwise noted. Absorption spectra were recorded on a HP 8452A diode-array spectrophotometer. Corrected steady-state emission measurements were conducted on a SPEX F-112 fluorimeter. Emission quantum yields were measured by relative actinometry, with 9,10-dicyanoanthracene ($\Phi_{em} = 0.89$) and perylene ($\Phi_{em} = 0.89$) in ethanol as actinometers.[54] Time-resolved emission decays were obtained by time-correlated single photon counting on an instrument that was constructed in-house. Excitation was effected by using either a pulsed LED source or a blue pulsed diode laser (IBH instruments, Edinburgh, Scotland). The pulsed LED and diode laser sources have pulse widths of ca. 1 ns. The time-resolved emission was collected using a red-sensitive, photon-counting PMT (Hamamatsu R928), and the light was filtered using 10 nm band-pass interference filters. Lifetimes were determined from the observed decays by using fluorescence lifetime deconvolution software. Low-temperature emission measurements were conducted in 1 cm diameter glass tubes contained in an Oxford Instruments DN1704 optical cryostat connected to an Omega CYC3200 automatic temperature controller. Nanosecond transient absorption spectra[55] and laser-induced optoacoustic spectroscopy (LIOAS) measurements[56] were obtained on previously described instrumentation, with the third harmonic of a Nd:YAG laser (355 nm, 10 ns fwhm, 5 mJ $pulse^{-1}$ {TA}, 8−30 μJ $pulse^{-1}$ {LIOAS}) as the excitation source. Primary factor analysis followed by first order (A → B) least-squares fits of the transient absorption data was accomplished with SPECFIT global analysis software (Spectrum Software Associates). LIOAS data (average of four data acquisitions) was obtained with both 1 and 5 MHz transducers, and deconvolution analysis of the LIOAS data was performed with Sound Analysis software (Quantum Northwest, Inc.). Picosecond transient absorption spectroscopy was carried out using instrumentation that has been previously described.[57−59]

Electrochemical Measurements. Electrochemical measurements were conducted on THF solutions with tetrabutylammonium hexafluorophosphate (TBAH, Aldrich) as the supporting electrolyte. Cyclic voltammetry was carried out on nitrogen bubble-degassed solutions (TBAH = 0.1 M) with a BAS CV-27 Voltammograph and MacLab Echem software. A GCE disk working electrode, platinum wire auxiliary electrode, and silver wire quasi-reference electrode were used, and potentials were corrected to values vs SCE via an internal standard (ferrocene, $E^{ox}_{1/2} = +0.40$ V vs SCE). A scan rate of 100 mV-sec^{-1} was employed in all measurements. Spectroelectrochemistry measurements were conducted in a custom cell on solutions degassed by four freeze−pump−thaw cycles (ca. 10^{-4} Torr; TBAH = 0.05 M). Platinum mesh working and auxiliary electrodes and a silver wire quasi-reference electrode were used. Absorption measurements on this cell were conducted in an Ocean Optics in-line filter holder connected to an Ocean Optics S2000 CCD-spectrometer by a UV-rated fiber optic cable (600 μm diameter) and a xenon arc lamp excitation source.

Time-resolved cw (continuous wave) EPR (TREPR) spectra were recorded with a Varian E9 X-band spectrometer with variable temperature accessory adapted for direct detection of EPR signals with a PAR model 162 boxcar averager.[60] Samples in a 1:1 toluene−chloroform glass at ∼130 K were excited with the third harmonic (355 nm, 10 mJ/pulse, 10 Hz) of a Quanta Ray GCR12 Nd:YAG laser. The boxcar detection window typically was set at 200−700 ns post flash.

(53) For comparison purposes, Re-2 and Re-3 (KCl pellet) exhibit stretches at 1902, 1927, and 2025 cm^{-1}. The shift of the ν_{CO} bands to higher frequency in **ReACN-2** and **Re-ACN-3** is consistent with substitution of Cl with η_1-$NCCH_3$.

(54) Murov, S. L.; Carmichael, I.; Hug, G. L. *Handbook of Photochemistry*, 2nd ed.; Marcel Dekker: New York, 1993.

(55) Wang, Y. S.; Schanze, K. S. *Chem. Phys.* **1993**, *176*, 305−319.

(56) Walters, K. A.; Schanze, K. S. *The Spectrum*; Newsletter of the Center for Photochemical Sciences; Bowling Green State University: Bowling Green, OH; http://www.bgsu.edu/departments/photochem/Summer1998Spectrum.pdf; 1998; Vol. 11, pp 1−4.

(57) Gosztola, D.; Yamada, H.; Wasielewski, M. R. *J. Am. Chem. Soc.* **1995**, *117*, 2041−2048.

(58) Greenfield, S. R.; Svec, W. A.; Gosztola, D.; Wasielewski, M. R. *J. Am. Chem. Soc.* **1996**, *118*, 6767−6777.

(59) Lukas, A. S.; Miller, S. E.; Wasielewski, M. R. *J. Phys. Chem. B* **2000**, *104*, 931−940.

(60) van Willigen, H.; Vuolle, M.; Dinse, K. P. *J. Phys. Chem.* **1989**, *93*, 2441−2444.

Scheme 2

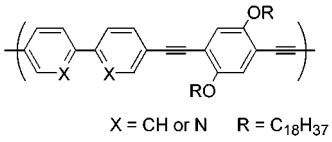

Results

Structures and Synthesis. This study examines the photophysical properties of the series of oligomeric aryleneethynylenes (OAEs) **1**−**4**, and the corresponding *fac*-(L)Re(CO)$_3$Cl complexes **Re-1**−**Re-4** (Scheme 1). Each oligomer contains a "core" consisting of a 5,5′-(2,2′-bipyridyl) unit. The primary repeat unit of the π-conjugated OAE chain is shown in Scheme 2. Including the 2,2′-bipyridine-5,5′-diyl unit, oligomers **1**−**4**, respectively, contain approximately 1.5, 2.5, 3.5, and 5.5 "repeat units" in the OAE chain.

The bipyridine containing oligomers were synthesized by an iterative sequence in which the key steps involved Pd-mediated cross coupling of a terminal acetylene and an aryl iodide (Sonogashira coupling).[52] The oligomers were characterized by ^{1}H and ^{13}C NMR and mass spectroscopy. The (L)Re(CO)$_3$Cl complexes **Re-1**−**Re-4** were prepared by reaction of Re(CO)$_5$Cl with the oligomer "ligand".[51] The metal complexes were also characterized by ^{1}H and ^{13}C NMR and FTIR spectroscopy. Details regarding the synthesis and spectral characterization of **1**−**4** and **Re-1**−**Re-4** were reported in a recent communication.[31]

The (L)Re(CO)$_3$(NCCH$_3$)$^+$ complexes **ReACN-2** and **ReACN-3** were prepared by reaction of the corresponding (L)Re(CO)$_3$Cl complexes with AgOTf in CH$_3$CN solution. The Cl-to-CH$_3$CN ligand exchange reactions were carried out on a very small scale, and consequently the **ReACN-2** and **ReACN-3** products were not characterized by NMR spectroscopy. However, the products were characterized by FTIR and mass spectroscopy. In addition, TLC analysis indicated that Cl-to-CH$_3$CN ligand exchange was quantitative in both cases.

Photophysics of Oligomers 1−4. UV−visible absorption spectra of **1**−**4** in THF solution are shown in Figure 1a, and the absorption maxima and molar absorptivities are listed in Table 1. The oligomers feature two absorption bands in the near-UV and visible regions. The low-energy band is due to the long-axis polarized π,π^* transition, while the higher-energy band is due to the short-axis π,π^* transition. Both absorption bands shift to significantly lower energy on going from **1** to **2**; however, the energy of the bands remains relatively constant for **2** to **4**. This trend indicates that the conjugation length is defined relatively early in the series. It is noteworthy that the absorption spectra of **3** and **4** are closely similar to those of structurally related OAEs and PPE polymers that have been previously reported.[18,22,23,25,26,61−65] Table 1 also lists the approximate molar absorptivity per repeat unit (see above for definition of repeat unit) for the lowest-energy absorption band in each oligomer. This parameter remains relatively constant across the series, indicating that to a first-order approximation the oscillator strength increases linearly with oligomer length.

All of the oligomers feature a strong blue fluorescence. Figure 2 illustrates the fluorescence spectra of **1**−**4** and Table 1 contains

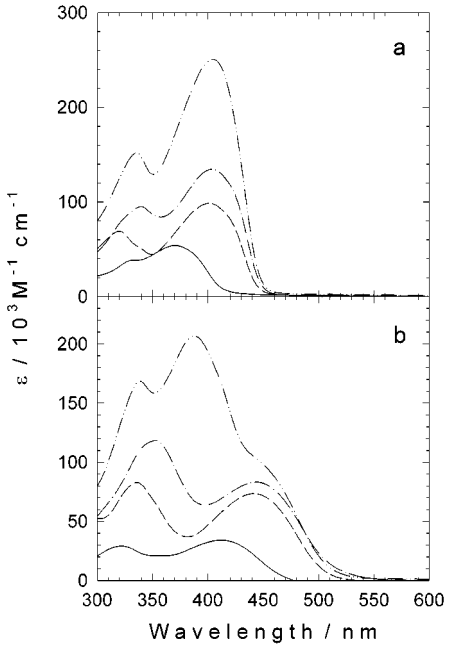

Figure 1. Absorption spectra for THF solutions. (a) **1**: (—); **2**: (- − -); **3**: (—•—); **4**: (—••—). (b) **Re-1**: (—); **Re-2**: (- − -); **Re-3**: (—•—); **Re-4**: (—••—).

a listing of the fluorescence quantum yields, lifetimes and radiative decay rates (ϕ_f, τ_f, and k_r, respectively). Comparison of the fluorescence spectra of the oligomers reveals that the spectral bandwidth decreases with increasing oligomer length. In addition, a clear trend emerges for oligomers **2**−**4**: the intensity of the 0,1 band relative to the 0,0 band decreases along the series **2** > **3** > **4**. This trend signals that the electron-vibration coupling in the $^1\pi,\pi^*$ state decreases with increasing oligomer length. The trend observed in the fluorescence bandwidth and vibronic structure for the oligomers implies that the $^1\pi,\pi^*$ state becomes more delocalized as the oligomer length increases.[13,14]

The fluorescence lifetimes of the oligomers range from 2.4 to 0.68 ns, and the general trend is that the lifetime decreases with increasing oligomer length. By contrast, the fluorescence quantum yield is highest for **1** and then is comparatively constant for the longer oligomers. The radiative decay rate, k_r, computed from the ratio ϕ_f/τ_f, gradually increases with increasing oligomer length. The experimentally observed k_r's are in reasonable agreement with those computed using the Strickler−Berg equation (k_r^{SB}, Table 1),[13] which confirms that the fluorescence emanates from the same state that gives rise to the lowest absorption band. In addition, the fact that the radiative decay rates are relatively large and close to those calculated with the Strickler−Berg relationship indicates that the fluorescence arises from a strongly allowed radiative transition. We infer this as a confirmation that in oligomers **1**−**4** the lowest excited state is of ^1B_u symmetry.[13,14]

Laser flash photolysis of **1**−**4** in THF solution at room temperature affords long-lived transient absorptions. For each oligomer the transients are very long-lived (τ > 150 μs, see Table 1) and are quenched by low-energy triplet energy acceptors (E_T < 50 kcal-mol^{-1}). On the basis of these observations we assign the long-lived transients to the $^3\pi,\pi^*$ excited states of the oligomers. The absorption difference spectra (triplet−triplet) for the $^3\pi,\pi^*$ states of **1**−**4** are shown in Figure 3. Each spectrum is characterized by strong bleaching of the ground-state absorption band (380−420 nm) and broad absorption throughout the visible region and continuing into the near-

(61) Swager, T. M. *Acc. Chem. Res.* **1998**, *31*, 201−207.
(62) Swager, T. M.; Gil, C. J.; Wrighton, M. S. *J. Phys. Chem.* **1995**, *99*, 4886−4893.
(63) Halkyard, C. E.; Rampey, M. E.; Kloppenburg, L.; Studer-Martinez, S. L.; Bunz, U. H. F. *Macromolecules* **1998**, *31*, 8655−8659.
(64) Bunz, U. H. F. *Chem. Rev.* **2000**, *100*, 1605−1644.
(65) Palmans, A. R. A.; Smith, P.; Weder, C. *Macromolecules* **1999**, *32*, 4677−4685.

Table 1. Photophysical Properties of Oligomers **1**−**4**[a]

	absorption		fluorescence					triplet state		
compound	λ_{max}/ nm	ϵ_{max}/ 10^3 M^{-1} cm^{-1} [b]	λ_{max}/ nm[c]	τ_f/ ns	ϕ_f	k_r/ 10^9 s^{-1}	k_r^{SB}/ 10^9 s^{-1}[d]	E_T/ kcal-mol^{-1}	ϕ_T[e]	τ_T/ μs[f]
1	330	38.5	455	2.4	0.89	0.37	0.65	52.3	0.05(1)	160
	370	54.0	(60.8)							
		(36.0)								
2	320	69.0	454	0.95	0.72	0.76	0.87	50.6	0.21(6)	450
	400	98.0	(63.0)							
		(39.2)								
3	340	95.0	453	1.1	0.68	0.61	1.2	50.6	0.26(3)	340
	404	135	(63.1)							
		(38.5)								
4	336	152	452	0.68	0.79	1.2	2.3	50.0	0.17(4)	410
	406	251	(63.3)							
		(46.0)								

[a] All data for argon-deoxygenated THF solutions. Errors: ϵ_{max} ±5000 M^{-1} cm^{-1}; τ_f ±0.4 ns; ϕ_f ±0.06; τ_T ±50 μs. [b] Number in parentheses is molar absorptivity per "repeat unit", see text. [c] Number in parentheses is fluorescence energy in kcal-mol^{-1}. [d] Calculated using Strickler−Berg equation (ref 13). [e] Number in parentheses is the experimental error (in the last digit). [f] Freeze−pump−thaw degassed solution.

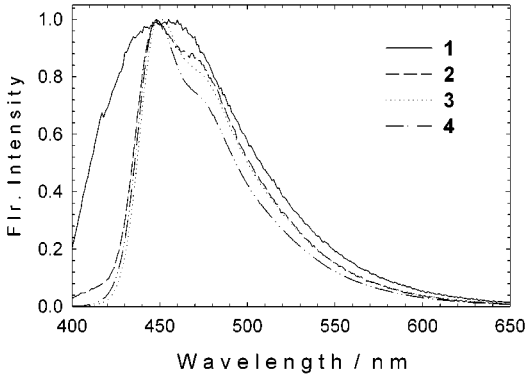

Figure 2. Fluorescence spectra of **1**−**4** in THF solution at 298 K. Excitation wavelength: 350 nm.

IR. The triplet−triplet spectra of oligomers **2**−**4** are remarkably similar to the triplet−triplet spectrum of a structurally related PPE polymer.[66]

The energies of the triplet states (E_T, Table 1) were determined by carrying out a series of Stern−Volmer quenching experiments on each oligomer using six triplet energy acceptors. The triplet energies were determined by fitting the resulting Sandros plots to a Marcus-type expression (see Supporting Information for the Sandros Plots).[66] Interestingly, the triplet energy of **2**−**4** is the same within experimental error (∼50 kcal-mol^{-1}); however, E_T for **1** is higher by a few kcal-mol^{-1}. Note also that E_T for the bipyridine-containing oligomers is very similar to the triplet energy of a structurally related PPE polymer (51.2 kcal-mol^{-1}).[66]

Time-resolved photoacoustic calorimetry was used to determine the triplet yields for oligomers **1**−**4**, and the resulting values are listed in Table 1.[56] Within experimental error, the triplet yields for **2**−**4** are approximately the same (∼20%). Furthermore, the sum of the fluorescence and triplet quantum yields ($\phi_f + \phi_T$) is close to unity, which indicates that photoexcitation of the oligomers leads almost exclusively to radiative decay or intersystem crossing (i.e., very little nonradiative decay occurs from the singlet excited state).

Absorption and Luminescence Properties of Re-1−Re-4. The UV−visible absorption spectra of **Re-1**−**Re-4** are shown in Figure 1b, and band maxima and molar absorptivity values are listed in Table 2. The spectrum of each metalated oligomer features at least two bands, one in the visible and a second, more intense band in the near UV. Interestingly, the wavelength maximum and oscillator strength of the visible absorption band is comparatively constant for the series **Re-2**−**Re-4**, while the higher energy band red-shifts and increases in oscillator strength across the series. This feature suggests that the low-energy band is associated with a chromophore that remains "constant" for **Re-2**−**Re-4**, while the higher energy bands arise from a segment of the molecule that is "varying" across the series. Although

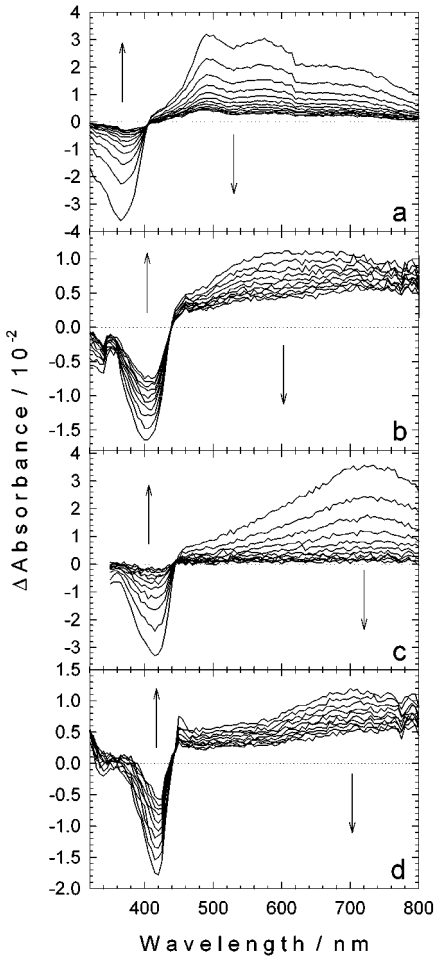

Figure 3. Transient absorption difference spectra of **1**−**4** in argon-deoxygenated THF solution at 298 K following 355 nm pulsed excitation. Spectra were acquired at 40 μs increments after laser excitation, and arrows indicate direction of change of ΔA with increasing time. (a) **1**. (b) **2**. (c) **3**. (d) **4**.

(66) Walters, K. A.; Ley, K. D.; Schanze, K. S. *J. Chem. Soc., Chem. Commun.* **1998**, *10*, 1115−1116.

Table 2. Photophysical and Electrochemical Properties of *fac*-(L)Re(CO)$_3$Cl Complexes[a]

	absorption		emission					
complex	λ_{max}/nm	ϵ_{max}/10^3 M^{-1} cm^{-1}	λ_{max}/nm 298 K	τ_i/ns (α_i)[b] 298 K	λ_{max}/nm 80 K	τ_i/ns (α_i)[b] 80 K	τ_{TA}/ns[c]	$E_{1/2}^{red}$/V[d]
Re-1	332	29.0	690	1.6 (0.93)	586	61 (0.53)	20	−0.88
	410	34.0		14 (0.07)		6240 (0.47)		
Re-2	336	83.0	650	2.0 (0.99)	659	2.4 (0.99)	145	−0.87
	440	73.4		154 (0.01)		2490 (0.01)		
Re-3	352	118	652	2.4 (0.99)	642	5.1 (0.99)	198	−0.86
	444	83.0		174 (0.01)		5110 (0.01)		
Re-4	338	168	650	3.8 (0.99)	642	7.7 (0.99)	161	−0.91[e]
	388	207		170 (0.01)		7610 (0.01)		
	444	103						
ReACN-2	340	94.9	652	0.18 (0.998)	589	0.36 (0.99)	9710[f]	−
	449	73.8		8.5 (0.002)	625	5.7 (0.01)		
ReACN-3	348	147	650	0.17 (0.997)	629	0.32 (0.99)	5010[f]	−
	447	94.9		9.2 (0.003)		5.7 (0.01)		
(bpy)Re(CO)$_3$Cl[g]	400[h]	2.4	642[h]	39[h]	540	3120	−	−1.35[i]
(bpy)Re(CO)$_3$(ACN)$^+$[f,j]	360	3.0	540	1100	−		−	−1.26[k]

[a] Room-temperature data for THF solutions and 80 K data for 2-MTHF glasses, unless otherwise noted. Errors: ϵ_{max} ±5000 M^{-1} cm^{-1}; τ_{em} ±10 ns; τ_{TA} ±10 μs. [b] Lifetimes and normalized amplitudes (in parentheses) obtained from two-component fits of emission decays according to the equation, $I(t) = \alpha_1 \exp\{-t/\tau_1\} + \alpha_2 \exp\{-t/\tau_2\}$. [c] Decay lifetime of transient absorption. [d] Reduction potential of metal−organic oligomer in THF/0.05 M TBAH solution, V vs SCE. [e] Irreversible reduction. [f] CH_2Cl_2 solution. [g] Data from ref 50. [h] 2-MTHF solution. [i] CH_3CN solution. [j] Data from ref 88. [k] DMF solution, data from ref 89.

we reserve a detailed discussion of the absorption spectra until a later discussion, at this point we note that the intensity of the low-energy absorption band for each oligomer is considerably stronger than expected if the transition is MLCT.[49] Therefore, all of the clearly resolved bands present in the absorption spectra of **Re-1**−**Re-4** are believed to arise from π,π^* "intraligand" transitions localized on the OAE. We infer that the Re → bpy-oligomer MLCT bands are "buried" under these considerably more intense π,π^* transitions.

The PL of **Re-1**−**Re-4** was carefully examined over the temperature range from 77 to 298 K with dilute ($c \approx 2-5$ μM) samples dissolved in 2-methyltetrahydrofuran (MTHF). First, all of the complexes feature only very weak emission in the region where fluorescence from the free oligomers is observed (400−550 nm). In most cases emission in this spectral region is more than 100-fold weaker compared to that of the free OAEs. Although the observed fluorescence may emanate from the metal−organic complexes, it is impossible to rule out the possibility that the emission does not originate from a trace amount of the unmetalated oligomers present in the samples. In any event, it is safe to conclude that fluorescence from the $^1\pi,\pi^*$ manifold is efficiently quenched by the metal complex chromophore in **Re-1**−**Re-4**.

By contrast, weak luminescence is observed for **Re-1**−**Re-4** in the 500−800 nm region. Figure 4 shows the PL spectra of each complex over the 77−298 K temperature range. For all of the complexes the room-temperature emission is very weak ($\phi \ll 0.005$). The emission intensity increases substantially upon cooling (a 20-fold increase on cooling from 298 to 77 K is typical) so that at low temperature the emission is moderate in intensity. Nonetheless, due to the low intensity of the room-temperature luminescence, quantum yield measurements were not attempted. At 298 K the emission of **Re-1** is characterized by a broad-structureless band with $\lambda_{max} = 680$ nm (see inset, Figure 4a). By contrast, at 77 K the emission is significantly blue-shifted ($\lambda_{max} = 586$ nm) and is highly structured, showing a clear vibronic progression with $\Delta\nu \approx 1350$ cm^{-1}. The emission spectra of **Re-2**−**Re-4** are similar to one another but differ from that of **Re-1**. First, at 77 K, the emission of the three complexes is distinguished by three "peaks" that are reasonably well-resolved in **Re-2** and **Re-3**, but less so in **Re-4**. Close inspection of the 77 K spectra of **Re-2** and **Re-3** suggests that these three

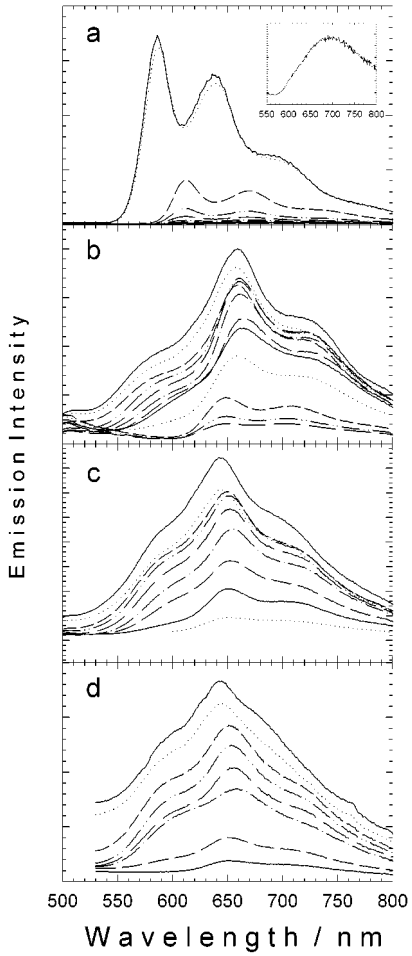

Figure 4. Temperature-dependent emission spectra of complexes **Re-1**−**Re-4** in a vacuum degassed 2-MTHF solution (glass). Temperatures are listed in order of decreasing emission intensity. (a) **Re-1**: $T = 80$, 100, 122, 140, 160, 180, 200, 220, 240, 260 K. (Inset) 280 K, spectrum normalized. (b) **Re-2**: $T = 81$, 103, 121, 141, 182, 204, 222, 240, 260, 280, 298 K. (c) **Re-3**: $T = 80$, 110, 128, 140, 160, 196, 222, 249, 298 K. (d) **Re-4**: $T = 81$, 110, 142, 170, 204, 230, 260, 298 K.

"peaks" arise from the superposition of a structureless emission band with λ_{max} between 580 and 600 nm, and a structured

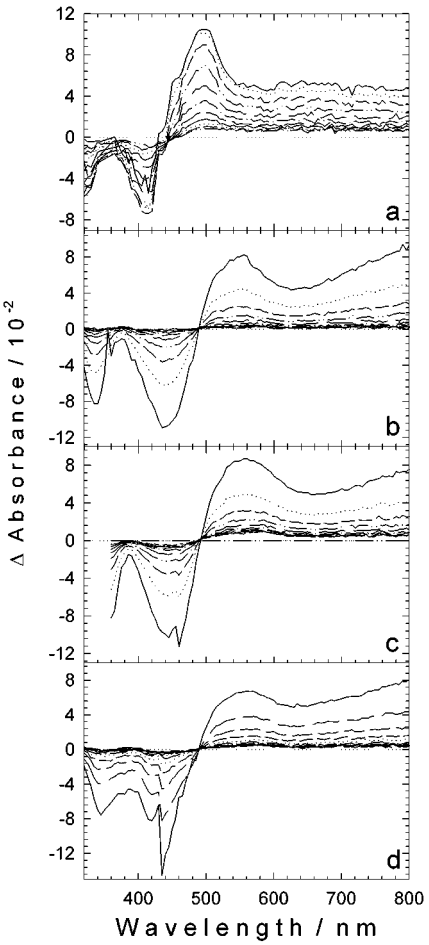

Figure 5. Transient absorption difference spectra of **Re-1**−**Re-4** in argon-deoxygenated THF solution at 298 K following 355 nm pulsed excitation. Spectra acquired at 4 ns increments for **Re-1** and at 80 ns increments for **Re-2**−**Re-4**. (a) **Re-1**. (b) **Re-2**. (c) **Re-3**. (d) **Re-4**.

emission with $\lambda_{max} \approx 650$ (the 0,0 band) nm and a vibronic sideband (the 0,1 band) that appears to the red of the main band. The emission intensity of **Re-2**−**Re-4** decreases in intensity with warming, but no significant shift in the position of the emission band is observed. Indeed, for all three complexes λ_{max} is virtually the same at 77 and 298 K. At 298 K the PL, although weak, is dominated by a structured band with $\lambda_{max} \approx 650$ nm.

The emission decay profiles of **Re-1**−**Re-4** are multiexponential. Table 2 contains a listing of parameters recovered from two-component fits of the emission decays for the complexes at 80 and 298 K. At 298 K the decays are characterized by a large amplitude, very short-lived component ($\tau \approx 1$ ns, $\alpha > 0.95$), and a low-amplitude component with a considerably longer lifetime ($\tau \approx 20-200$ ns) that varies somewhat with oligomer length. At 80 K in a rigid solvent glass the decays are qualitatively similar. In each case the lifetime of the short-lived decay component remains almost the same; however the lifetime of the long-lived component increases significantly.

Transient Absorption of Metal−Oligomers Re-1−Re-4. Nanosecond laser flash studies were carried out on **Re-1**−**Re-4** using the third harmonic of a Nd:YAG laser for excitation ($\lambda = 355$ nm, 10 ns fwhm). In all cases, strongly absorbing transients with lifetimes in the 10−200 ns time domain were observed. Figure 5 illustrates time-resolved transient absorption (TA) difference spectra for the four complexes. The TA decay lifetimes (τ_{TA}), obtained from global kinetic analysis of the time-resolved spectral data, are listed in Table 2. As can be seen in Figure 5, the absorption difference spectrum for each of the

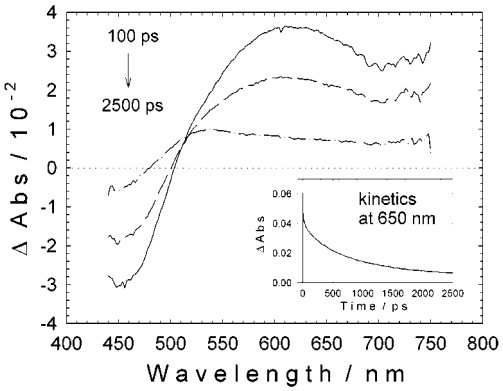

Figure 6. Picosecond transient absorption difference spectra for **Re-4** in THF solution following 400 nm excitation (80 fs pulse width). (—) 100 ps delay; (– – –) 500 ps delay, (–•–) 2500 ps delay.

complexes is characterized by: (1) bleaching of the ground-state absorption bands in the 350−450 nm region, (2) a strong mid-visible absorption band in the 500−550 nm region, and (3) a broad, featureless absorption in the red that continues into the near-IR region. It is interesting to note that the dominant feature in all of the spectra is the bleach/absorption feature in the 400−550 nm region. This derivative-shaped feature suggests that the position of the lowest-energy π,π^* transition is red-shifted in the excited state (relative to the ground state). The lifetime of **Re-1** is rather short ($\tau \approx 20$ ns); however, the transients observed for the longer oligomers decay with comparable lifetimes of 150−200 ns. Note that there is a strong correlation between the lifetimes of the transients observed by ns flash photolysis and the long-lived emission decay component (compare lifetimes in Table 2). This correspondence suggests that the TA arises from the emitting excited state, or alternatively it is an excited state that is in equilibrium with the luminescent state.[67−73]

A limited series of studies were carried out to characterize the TA properties of the metal−organic oligomers on the picosecond time scale. The observations made with **Re-4** are typical of those seen for the oligomers and therefore we only present data for this complex herein. Figure 6 shows absorption difference spectra obtained for **Re-4** in THF solution at 100, 500 and 2500 ps following 400 nm pulsed excitation (80 fs pulse width), and the inset shows the transient absorption decay kinetics monitored at 650 nm. As can be seen from the data, there is clearly a relaxation occurring on the ps time scale following initial excitation of the complex. Analysis of the kinetic data reveals the following: (1) an ultrafast decay ($\tau \approx 16$ ps), (2) a "slower" relaxation process with $\tau \approx 770$ ps, (3) a transient absorption that persists into the nanosecond time domain. Inspection of the time-resolved difference spectra shows that on the 100−2500 ps time scale there are only minor changes

(67) Shaw, J. R.; Webb, R. T.; Schmehl, R. H. *J. Am. Chem. Soc.* **1990**, *112*, 1117−1123.
(68) Shaw, J. R.; Schmehl, R. H. *J. Am. Chem. Soc.* **1991**, *113*, 389−394.
(69) Simon, J. A.; Curry, S. L.; Schmehl, R. H.; Schatz, T. R.; Piotrowiak, P.; Jin, X.; Thummel, R. P. *J. Am. Chem. Soc.* **1997**, *119*, 11012−11022.
(70) Baba, A. I.; Shaw, J. R.; Simon, J. A.; Thummel, R. P.; Schmehl, R. H. *Coord. Chem. Rev.* **1998**, *171*, 43−59.
(71) Schmehl, R. H. *The Spectrum*; Newsletter of the Center for Photochemical Sciences; Bowling Green State University: Bowling Green, OH; http://www.bgsu.edu/departments/photochem/; 2000; Vol. 13, pp 17−21.
(72) Tyson, D. S.; Castellano, F. N. *J. Phys. Chem. A* **1999**, *103*, 10955−10960.
(73) Tyson, D. S.; Bialecki, J.; Castellano, F. N. *Chem. Commun.* **2000**, 2355−2356.

in the spectral band shape—the dominant process that occurs on this time scale is associated with the loss of a significant fraction of the initial TA amplitude. Nonetheless, there is a blue-shift in the transient absorption band (610 nm → 530 nm) occurring on this time scale. Note that the spectrum observed for **Re-4** at "long times" (i.e., 2500 ps delay) in the picosecond pump−probe experiment corresponds well with the transient absorption difference spectrum observed by nanosecond flash photolysis (compare Figures 5d and 6). Finally, there is reasonable correspondence between the lifetime of the intermediate decay component seen in the picosecond pump−probe experiment ($\tau \approx 770$ ps) and the fast component observed in the emission decay experiments. This fact suggests that the sub-ns time scale dynamics that are observed by PL and transient absorption may arise from the same physical relaxation process.

Electrochemistry and Spectroelectrochemistry of Re-1−Re-4. Cyclic voltammetry was carried out on the metal−organic oligomers in an effort to determine the potentials for oxidation and reduction of the complexes. Owing to the poor solubility of the oligomers in polar solvents typically used for electrochemistry, these studies were limited to CH_2Cl_2 and THF solution. After extensive trial-and-error, it was found that the optimal conditions for CV were obtained in THF solution with a glassy carbon working electrode.[74] Under these conditions, reversible one-electron reduction waves were observed for the first reduction of **Re-1**−**Re-3**, while the first reduction of **Re-4** was quasi-reversible (unsymmetrical anodic and cathodic waves). For each of the complexes the reduction occurs with $E_{1/2} \approx -0.90$ V vs SCE (see Table 2). Unfortunately, sweeps to positive potentials were limited by the accessible potential window in THF (anodic limit $\approx +1.4$) and therefore it was not possible to obtain potentials for oxidation of the complexes.

Quite clearly the first reduction of **Re-1**−**Re-4** arises from one-electron reduction of the metalated oligomer. Given that the reduction potential does not shift significantly across the series, we conclude that the anion radical is localized primarily on the 2,2′-bipyridine "segment" of the conjugated oligomer (i.e., the LUMO of the oligomer has the highest density on the metal−bipyridine unit). Nonetheless, the first reduction potentials of **Re-1**−**Re-4** are considerably less than those for the parent complex (bpy)Re(CO)$_3$Cl (−1.35 V),[50] which indicates that the aryl-ethynyl moieties that are at the 5,5′ positions on the bipyridine stabilize the reduced complex (i.e., the LUMO energy is reduced by the π-conjugation). This further implies that in the reduced complex there is some delocalization of electron density into the appended aryl-ethynyl units.

Spectroelectrochemistry was carried out on solutions of **Re-3** and **Re-4** to obtain information concerning the absorption of the reduced complexes. Figure 7 illustrates the spectra obtained when vacuum degassed solutions of the complexes were reduced at a potential negative of the first reduction wave observed by CV. In each case the original spectrum could be reproduced when the solution was reoxidized by switching the potential back to 0 V, suggesting that the species observed in the spectroelectrochemistry arises from one-electron reduction of the complex. For both complexes, reduction results in bleaching of the lowest energy absorption band ($\lambda \approx 450$ nm) with a concomitant increase in the absorption in the red. It is important to notice that for **Re-4** the strong absorption band at $\lambda = 395$ nm is hardly affected by the reduction, suggesting that the chromophore involved in this optical transition is not affected significantly by the electrochemical reduction. This observation is consistent with the idea that the long-wavelength ground-state absorption band arises from absorption in the "bpy" core of the OAE oligomer and that the shorter wavelength bands arise from the OAE "periphery" (further discussion of this point is presented below).

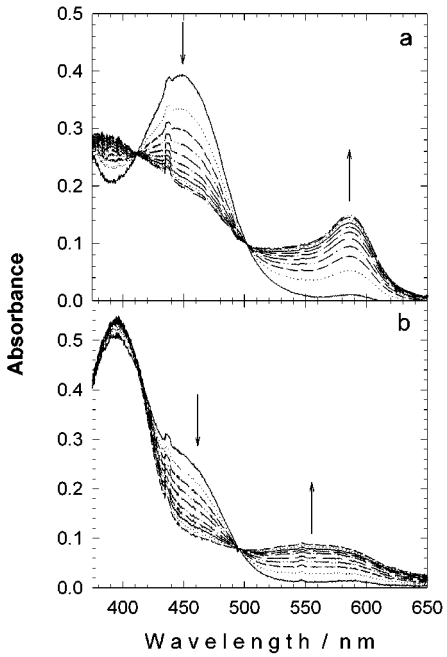

Figure 7. Spectroelectrochemistry of (a) **Re-3** and (b) **Re-4**. The samples were dissolved in THF/0.05 M TBAH and vacuum degassed. Spectra obtained at 2 min intervals after the working electrode was stepped to −1.2 V (**Re-3**) or −1.7 V (**Re-4**) vs SCE. Arrows indicate the direction of change with increasing electrolysis time.

Photophysics of ReACN Complexes. In an effort to provide further information concerning the nature of the lowest excited states in the metal−OAE complexes, the photophysics of **ReACN-2** and **ReACN-3** were examined. These complexes are analogues of **Re-2** and **Re-3** wherein the Cl ligand is replaced by η_1-NCCH$_3$. The CH$_3$CN complexes were prepared because it is known from work on the "parent" bipyridine complexes that substitution of Cl with NCCH$_3$ strongly influences the photophysics of the complex. Specifically, replacement of Cl with CH$_3$CN typically has the following effects:[50,51] (1) the energy of the MLCT state increases by 0.3−0.4 eV, and (2) the emission quantum yield and lifetime increase by 1−2 orders of magnitude. These effects are clearly illustrated by comparing the photophysical parameters of (bpy)Re(CO)$_3$Cl with those of (bpy)Re(CO)$_3$(NCCH$_3$)$^+$ (see Table 2). On the basis of these "typical" effects, it was anticipated that Cl-to-CH$_3$CN ligand exchange in the metal−OAEs would afford materials that are strongly luminescent and have longer excited-state lifetimes compared to those of **Re-1**−**Re-4**. Moreover, observation of the anticipated shift in the emission energy would provide evidence that the luminescence of the metal−oligomers emanates from the MLCT manifold.

Table 2 contains a listing of various photophysical parameters for the two CH$_3$CN complexes, **ReACN-2** and **ReACN-3**, and Figures 8 and 9 illustrate their temperature-dependent emission spectra and room-temperature TA spectra. First, the absorption spectra of **ReACN-2** and **ReACN-3** are nearly indistinguishable from those of the corresponding Cl-substituted complexes (see Table 2 to compare the absorption maxima). This is not

(74) In other solvents, the electrochemistry of the oligomers was found to be irreversible, presumably due to precipitation and adsorption of the reduced complex onto the electrode surface. Even in THF solution, it was often observed that a good CV could be obtained only on the first sweep. On successive scans the peak current would diminish, and the degree of reversibility of the electrode process would decrease.

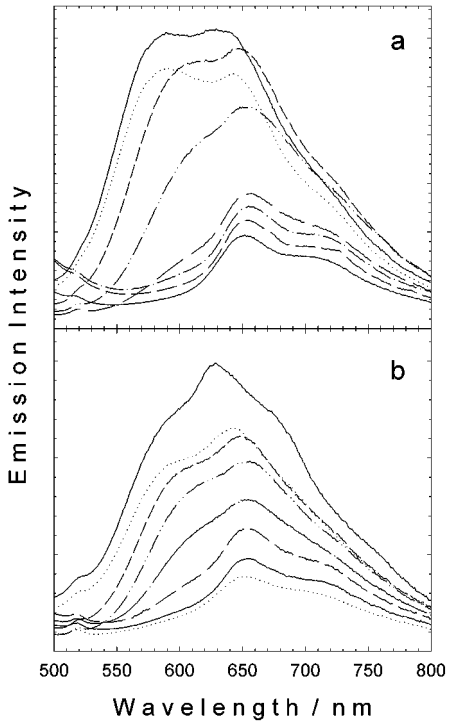

Figure 8. Temperature-dependent emission spectra of complexes **ReACN2** and **ReACN3** in a vacuum degassed 2-MTHF solution (glass). Temperatures are listed in order of decreasing emission intensity. (a) **ReACN2**: $T = 81$, 110, 140, 170, 199, 230, 260, 298 K (b) **ReACN3**: $T = 80$, 113, 140, 169, 200, 232, 259, 298 K.

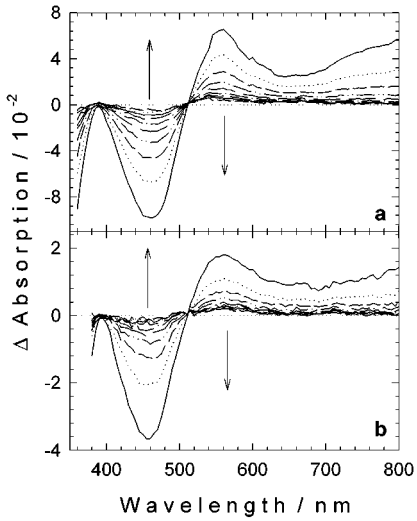

Figure 9. Transient absorption difference spectra of **ReACN2** and **ReACN3** in argon-deoxygenated CH_2Cl_2 solution at 298 K following 355 nm pulsed excitation. Spectra acquired at 4 μs increments and arrows indicate direction of change of ΔA with increasing time. (a) **ReACN2**. (b) **ReACN3**.

surprising, given that the absorption is dominated by π,π^* transitions localized on the oligomers. However, contrary to expectations, the PL of **ReACN-2** and **ReACN-3** is very weak, both at room temperature in CH_2Cl_2 solution and at 80 K in 2-MTHF ($\phi_{em} < 0.005$, see Table 2 and Figure 8). In addition, room-temperature emission maxima for the two CH_3CN complexes are very similar to their Cl counterparts. This latter feature is contrary to the expected emission blue-shift, and suggests that the room-temperature PL from **ReACN-2** and **ReACN-3** does not emanate from the MLCT manifold. Upon cooling to 80 K, the PL intensity from **ReACN-2** and **ReACN-3** increases modestly, and the spectra broaden significantly. The most noticeable effect is that at low temperature the emission of the two complexes appears as if it consists of two superimposed emission bands, one with an energy that is similar to that observed at room temperature ($\lambda_{max} \approx 640$ nm) and a second, new band that appears at higher energy ($\lambda_{max} \approx 575$ nm). Finally, consistent with the low emission intensities, emission decay experiments indicate that the decay time of the luminescence from **ReACN-2** and **ReACN-3** is very short at all temperatures (Table 2). This contrasts sharply with the emission decay kinetics of the Cl complexes, where a low-amplitude but long-lived decay component is observed at ambient temperature.

TA spectra obtained on **ReACN-2** and **ReACN-3** are illustrated in Figure 9. Note that the absorption difference spectra of the two CH_3CN complexes are *very* similar in appearance to those of the corresponding Cl complexes (compare with Figure 5). This strongly suggests that the nature of long-lived transients detected by transient absorption is the same, regardless if the ancillary ligand is Cl or CH_3CN. However, the unusual feature is that the lifetimes of the transients observed by transient absorption for **ReACN-2** and **ReACN-3** are considerably longer than those of **Re-1**−**Re-4** (see Table 2). It is also noteworthy that the transient absorption lifetimes for **ReACN-2** and **ReACN-3** are several orders of magnitude longer than their emission decay lifetimes. This feature makes it clear that the emission emanates from an excited state that is unique from that observed by TA.

Time-Resolved Electron Paramagnetic Resonance (TREPR). In an effort to gain further information on the nature of the long-lived transients observed following excitation of the metal−organic oligomers, TREPR experiments were carried out on selected oligomers and metal−oligomers. In these experiments the compounds were excited at 355 nm using a Nd:YAG laser, and the TREPR spectra were detected ∼500 ns after laser excitation. The objective of these experiments was to use EPR to confirm that the long-lived transients observed by flash photolysis are the $^3\pi,\pi^*$ states based on the π-conjugated system. All measurements were performed on samples in frozen solution at 130 K, because modulation of the dipole−dipole interaction between the unpaired electrons in a triplet generally broadens the EPR signals beyond detection in liquid solution.

The initial TREPR experiments were carried out using several of the free oligomers (i.e., **2**−**4**), however, in these measurements no signals were detected. At first this was a surprise, given that the ambient temperature photophysical studies on **2**−**4** indicate that the $^3\pi,\pi^*$ state is formed in moderate yield (Table 1). However, after discovering the EPR result, a transient absorption study was carried out on OAE **3** at 100 K. This experiment failed to detect the absorption of the $^3\pi,\pi^*$ state, indicating that this state is quenched in the low temperature glass. Previously reported fluorescence studies of **3** and **4** show that in dilute solution these compounds aggregate at $T < 200$ K.[75] Thus, the quenching of the $^3\pi,\pi^*$ state in **3** at low-temperature is believed to arise due to the aggregation. This triplet quenching mechanism accounts for the fact that an EPR signal is not detected for the free oligomers.

Further attempts to detect the TREPR spectrum of the $^3\pi,\pi^*$ state in an OAE were carried out using oligomer **5** (see Figure 10 for structure). Compound **5** was selected for the low-temperature FT-EPR experiment because laser flash photolysis of the compound at 100 K revealed the characteristic transient absorption of the $^3\pi,\pi^*$ state.[66] As shown in Figure 10, the

(75) Walters, K. A.; Ley, K. D.; Schanze, K. S. *Langmuir* **1999**, *15*, 5676−5680.

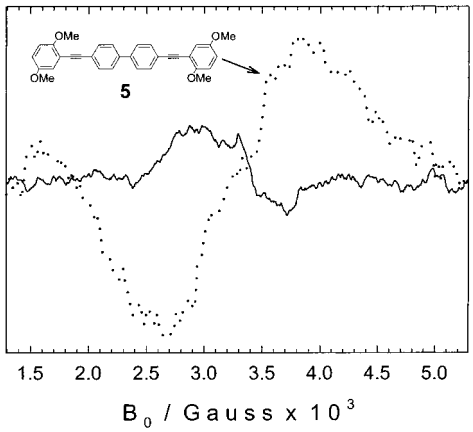

Figure 10. TREPR spectra of compound **5** (dotted line) and **ReACN2** (solid line) in toluene-chloroform (1:1) at 130 K. Delay between laser excitation and detection was ~500 ns.

TREPR spectrum of **5** at 130 K reveals a broad resonance ($g \approx 2$, peak-to-peak width $\approx$ 1200 G) which is observed at delay times <5 μs after the 355 nm excitation pulse. The signal is spin polarized with the low field half in emission (E) and the high field in absorption (A). The EPR signal is clearly due to the $^3\pi,\pi^*$ state, and the characteristic EA pattern arises from spin-polarization that is generated by the spin-selective singlet-to-triplet intersystem crossing step.[76] Next, TREPR experiments were carried out on **ReACN-2** at 130 K. Interestingly, a resonance with $g \approx 2$ is also observed for this metal−organic complex. However, in this case the resonance is less intense and not as broad as that observed for model **5** (for **ReACN-2** the peak-to-peak width is ~700 G). More importantly, the signal for **ReACN-2** exhibits an AE polarization (low field absorption, high field emission), which is opposite to the EA pattern observed for model **5**.

The TREPR resonance observed for **ReACN-2** is also likely due to an oligomer based $^3\pi,\pi^*$ state. This conclusion is based on the fact that an MLCT state would have a large contribution from Re-based d orbitals, and consequently the EPR resonance would be expected to have a g value that is shifted significantly from the free electron value. Moreover, an EPR signal would probably not be observed at all for an MLCT state, since spin−lattice relaxation would be exceedingly fast so that any spin polarization would vanish prior to detection of the signal. The fact that an AE pattern is observed for **ReACN-2**, while an EA pattern is observed for **5**, suggests that in the metalated oligomer the $^3\pi,\pi^*$ state is produced by a route other than direct singlet-to-triplet intersystem crossing. As discussed below, this pathway may involve the intermediacy of a ^{3}MLCT state.

The field range covered by the resonance peaks is a measure of the strength of the dipole−dipole interaction between the unpaired electrons in the triplets. The interaction is proportional to $\langle R^{-3} \rangle$ where R is the average distance between the unpaired electrons. The pronounced reduction in spectral width observed upon going from **5** to **ReACN-2** points to a contribution of the bipyridine ligand to the orbital of the unpaired electrons.

Discussion

Photophysics of Oligomers 1−4. Several previous studies have examined the absorption and fluorescence properties of PPE-type oligomers and polymers.[18,22,23,25,26,61−65] These studies have demonstrated that the lowest-energy absorption is strongly allowed and long-axis polarized. In addition, PPE materials typically feature short-lived fluorescence with high quantum yields (>0.50 is typical), which implies that the lowest singlet state is also strongly allowed. Taken together, this information implies that the lowest excited state in these systems is of ^1B_u character.

Most previous studies of PPE conjugated systems have examined materials in which the repeat unit consists of either 2-alkyl-1,4-phenyleneethynylene or 2,5-bisalkoxy-1,4-phenyleneethynylene moieties. In these systems the conjugation length, as assessed by the shift of the absorption or fluorescence maximum, continues to increase for oligomers having >10 phenyleneethynylene repeats and levels off as the number tends to 16.[26,77] This result suggests that the conjugation length of PPE materials that contain only 1,4-phenyleneethynylene repeats is at least 10 repeat units. West and co-workers reported that the absorption and fluorescence maxima of polymers with structures consisting of alternating 2,5-bisalkoxy-1,4-phenyleneethynylene and 1,4-phenyleneethynylene repeat units were approximately 415 and 450 nm, respectively.[78]

As noted above, the absorption and fluorescence properties of oligomers **2−4** are very similar to those of other PPE oligomers and polymers. This point indicates that the bipyridine unit does not significantly perturb the properties of the lowest $^1\pi,\pi^*$ excited state in **2−4**. However, an important feature with respect to **2−4** is that the maximum of the lowest-energy absorption band red-shifts only very slightly with increasing oligomer length, which indicates that the conjugation length is reached early in the series. This is surprising in view of the results obtained by other groups on PPE oligomers that suggest that the conjugation length is not established until $n > 10$. The restricted conjugation length in **2−4** likely arises because the 1,4′-biphenylene unit effectively disrupts the conjugation, owing to twisted inter-ring geometry (Scheme 3, top). The conclusion that the biphenylene unit disrupts conjugation is supported by the fact that the conjugation length in *p*-phenylene oligomers is ~40% shorter than in PPEs.[27]

Although the absorption spectra imply that the conjugation length is similar in **2−4**, there is an easily discernible change in the fluorescence band shape which indicates that the relaxed $^1\pi,\pi^*$ excited-state experiences a greater degree of delocalization with increasing oligomer length. Recent studies of intramolecular energy transfer in ethynylene-linked porphyrins indicate that inter-chromophore singlet energy transfer occurs on the 10−100 ps time scale, even when the process is isothermal.[79,80] On the basis of these results, we anticipate that due to its long lifetime ($\tau \approx 1$ ns), the $^1\pi,\pi^*$ excited state in **2−4** effectively samples the entire oligomer. This rapid exciton diffusion likely is responsible for the decreased electron-vibrational coupling which gives rise to the change in fluorescence band shape with increasing oligomer length.

The transient absorption and photoacoustic calorimetry studies of **1−4** indicates that in each case direct excitation of the oligomers leads to moderate yields of the $^3\pi,\pi^*$ state. Moreover, the triplet energy is comparatively constant across the series, consistent with the finding that the conjugation length is defined early in the series. The singlet−triplet (S−T) splitting in **1−4** is ~0.55 eV (4430 cm^{-1}), which is significantly less than that

(76) Sixl, H.; Schwoerer, M. Z. *Z. Naturforsch.* **1970**, *25A*, 1383.
(77) Pearson, D. L.; Tour, J. M. *J. Org. Chem.* **1997**, *62*, 1376−1387.
(78) Li, H.; Powell, D. R.; Hyashi, R. K.; West, R. *Macromolecules* **1998**, *31*, 52−58.
(79) Li, F. R.; Yang, S. I.; Ciringh, Y. Z.; Seth, J.; Martin, C. H.; Singh, D. L.; Kim, D. H.; Birge, R. R.; Bocian, D. F.; Holten, D.; Lindsey, J. S. *J. Am. Chem. Soc.* **1998**, *120*, 10001−10017.
(80) Kuciauskas, D.; Liddell, P. A.; Lin, S.; Johnson, T. E.; Weghorn, S. J.; Lindsey, J. S.; Moore, A. L.; Moore, T. A.; Gust, D. *J. Am. Chem. Soc.* **1999**, *121*, 8604−8614.

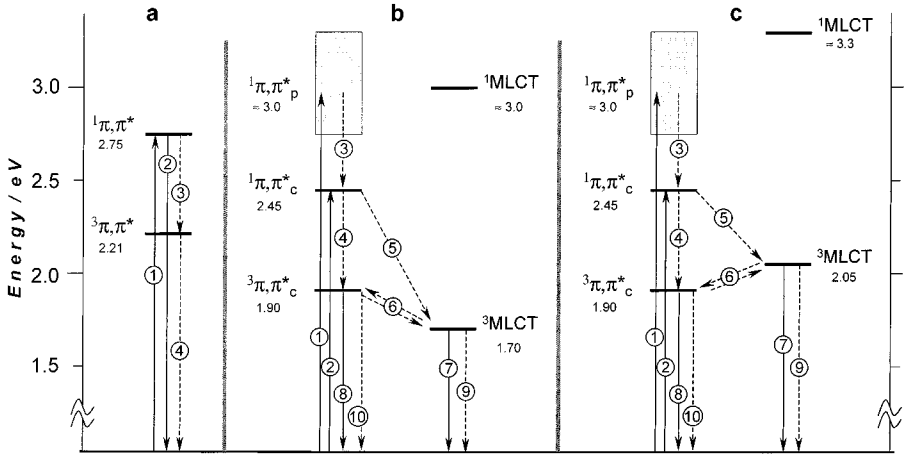

Figure 11. Jablonski Diagrams for: (a) free oligomers **1**−**4**; (b) metal−oligomers **Re-2**−**Re-4**; (c) metal−oligomers **ReACN-2** and **ReACN-3**. Solid and dashed lines indicate radiative and nonradiative transitions, respectively. Processes are labeled using numbers for ease of reference in the text.

Scheme 3

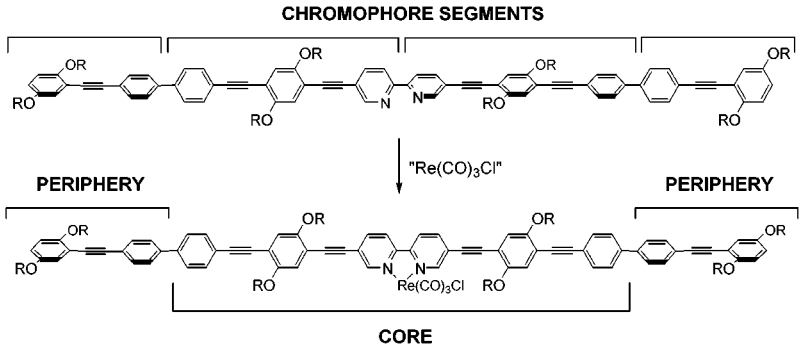

of the "parent chromophores" diphenyl acetylene (1.39 eV) and biphenyl (1.30 eV),[54] presumably because of the delocalized nature of the singlet and triplet states in the π-conjugated systems. However, it is surprising that the S−T splitting in the OAEs is also considerably less than that of other well-studied π-conjugated systems such as α-septithiophene (0.90 eV)[14] and MEH−PPV (0.72 eV).[81] The reason that the S−T splitting is lower in the OAEs compared to that in these other π-conjugated systems is unclear at the present time.

In previously published work we demonstrated that the spectroscopy and photophysics of oligomers **3** and **4** are strongly influenced by intrachain conformations (i.e., the phenylene-ethynylene-phenylene "ring−ring" torsion angles) and intramolecular aggregation.[75] In particular, the fluorescence spectra and polarization from dilute solutions of these oligomers display a strong temperature dependence. At intermediate temperatures (200−300 K), spectral changes are believed to arise from changes in intrachain conformation, while at lower temperatures (T < 200 K) the spectral (and polarization) changes are dominated by the presence of intermolecular aggregates. Although these effects have not been considered in the present report, we point them out to make it clear that intrachain conformation and interchain aggregation effects may play a role in the temperature-dependent photophysics of the metal complexes **Re-1**−**Re-4**.

The Jablonski diagram in Figure 11a summarizes the photophysics of OAEs **2**−**4**. The absorption, fluorescence and ns−μs transient absorption spectroscopy of the oligomers are dominated by the lowest $^1\pi,\pi^*$ and $^3\pi,\pi^*$ excited states which lie at 2.75 and 2.21 eV, respectively. Excited-state decay is dominated by fluorescence, with $S_1 \rightarrow T_1$ intersystem crossing being the second most efficient decay process from the $^1\pi,\pi^*$ manifold. Phosphorescence is not observed from any of the oligomers (77 K in 2-MTHF, 1 M ethyl iodide added). We believe the lack of phosphorescence may be due to the propensity of the oligomers to aggregate at low temperature, which leads to quenching of the $^1\pi,\pi^*$ state (and therefore reducing the triplet yield).

Metal−Organic Oligomers: Absorption Spectra. As indicated previously, the dominant feature in the UV−visible absorption spectra of **Re-2**−**Re-4** is the intense absorption band with $\lambda_{max} \approx 440$ nm and $\epsilon \approx 70\,000$ M^{-1} cm^{-1} (a similar band appears slightly blue-shifted and with a smaller ϵ in **Re-1**). This band is obviously associated with the $-Re(CO)_3Cl$ unit; however, for the reasons outlined below it is clear that the band arises from an OAE-based π,π^* transition, not Re → bpy-oligomer MLCT. First, although complexes of the type (diimine)-$Re(CO)_3Cl$ typically feature an MLCT absorption band in the 400−450 nm region,[50] the MLCT band is only weakly allowed with $\epsilon \approx 2000-4000$ M^{-1} cm^{-1} (cf. Table 2). Thus, the 445 nm absorption band in **Re-2**−**Re-4** is too intense to be due to Re → bpy-oligomer MLCT. Second, in previous studies of PPE, PPV, and polythiophene polymers that contain 2,2′-bipyridine-5,5′-diyl chromophore, complexation with a variety of metals (including the closed shell Zn(II) ion) induces a 40−50 nm red-shift in the lowest-energy π,π^* transition of the conjugated system.[33−35,45] Recently published semi-empiricial studies suggest that metal-complexation of the bpy unit decreases the HOMO−LUMO gap of the π-system due to the following factors.[82] (1) Metal complexation forces the bipyridine rings

(81) Scurlock, R. D.; Wang, B.; Ogilby, P. R.; Sheats, J. R.; Clough, R. L. *J. Am. Chem. Soc.* **1995**, *117*, 10194−10202.

into a syn, planar conformation, effectively increasing the interring π-conjugation. (2) Interaction between the dπ metal orbitals and the bpy π-system lowers the energies of both the π and π^* levels; however, this effect is more pronounced for the π^* orbital which results in a decreased $\pi-\pi^*$ gap.[82]

While the low-energy absorption band is relatively constant in energy and intensity across the series **Re-2**−**Re-4**, all of the complexes feature a second intense band in the near-UV that red-shifts and increases in intensity significantly as the oligomer length increases. This property suggests that **Re-2**−**Re-4** essentially feature *two* oligomer-based chromophores we refer to as "core" and "periphery" (refer to Scheme 3). First, the low-energy absorption band is associated with the core chromophore consisting of the bipyridine moiety and four flanking phenyleneethynylene units (two on each side of the bipyridine). Importantly, all of the phenylene rings in the core are able to attain the coplanar conformation that facilitates π-delocalization. This core is present in each of **Re-2**−**Re-4**, which explains why the position and intensity of the long-wavelength absorption band is the same in these complexes. Second, the higher-energy π,π^* transition is associated with the periphery chromophore of the OAE oligomer system (Scheme 3). The energy and intensity of the transition associated with the periphery chromophore varies along the series **Re-2**−**Re-4** because the length of this chromophore varies substantially in this series.

Although the metal−organic oligomers do not fluoresce, based on the absorption shift that accompanies metalation (i.e., 400 nm → 445 nm), we estimate that the relaxed $^1\pi,\pi^*$ state for the core chromophore in **Re-2**−**Re-4** is approximately 0.3 eV lower in energy compared to the relaxed (fluorescent) $^1\pi,\pi^*$ state in the free oligomers. Moreover, assuming that the S−T splitting is unaffected by metalation, we estimate that the energy of the $^3\pi,\pi^*$ state of the core chromophore in **Re-2**−**Re-4** will also be lowered by ∼0.3 eV relative to that of the free oligomers. This estimate suggests that the lowest $^3\pi,\pi^*$ state in **Re-2**−**Re-4** should be approximately 1.90 eV (652 nm). Interestingly, this estimate corresponds exactly to the observed emission energy of the metalated oligomers, which strongly supports the premise that the structured emission emanates from the $^3\pi,\pi^*$ state of the core chromophore.

Excited-State Energetics. Before turning to an interpretative discussion of the remaining photophysical data, it is necessary to establish the energies for the various low-lying excited states in the OAEs. This presentation centers on complexes **Re-2**−**Re-4**, **ReACN-2** and **ReACN-3**, because the energetics for these systems are believed to be related. (The properties of **Re-1** are considered in a later section.) Figure 11 provides Jablonski diagrams for the free OAEs and the two categories of metal−OAE complexes. First, consider the situation for the free oligomers (**2**−**4**, Figure 11a). Each of these molecules features a $^1\pi,\pi^*$ state at 2.75 eV (based on the fluorescence) and a $^3\pi,\pi^*$ state at 2.21 eV (based on triplet quenching).

Next consider the excited-state diagram for the Cl-substituted complexes, **Re-2** - **Re-4** (Figure 11b). In this series, at least three excited states associated with the OAE π-system are identified. (1) The high-energy singlet, $^1\pi,\pi^*_p$, arises from the periphery OAE units. The energy of this state lies in the region of 2.7−3.3 eV (it varies with oligomer length). (2) The lowest-energy singlet state, $^1\pi,\pi^*_c$, is associated with the OAE core. The energy of this state is estimated as outlined in the previous section, and it is not expected to vary significantly with oligomer length. (3) The lowest triplet state, $^3\pi,\pi^*_c$, is also associated with the OAE core. The energy of this state is ∼1.90 eV based on the position of the weak phosphorescence band.

It is more problematic to pinpoint the energies of the ^{1}MLCT and ^{3}MLCT states in **Re-2** - **Re-4**, because the MLCT absorption(s) are obscured by the OAE-based π,π^* bands and the luminescence spectra are complicated. Thus, in the absence of direct spectroscopic evidence, the state energies are estimated on the basis of two facts. (1) The energies of the ^{1}MLCT and ^{3}MLCT states of the parent complex, (bpy)Re(CO)$_3$Cl are ∼3.3 and 2.0 eV, respectively. (2) The energies of the MLCT manifold in **Re-2**−**Re-4** will scale with the difference in reduction potentials between the oligomer complexes and (bpy)Re(CO)$_3$Cl.[50] The difference in these reduction potentials is ∼0.3 ± 0.1 V[83] On the basis of these facts, we estimate that the ^{1}MLCT and ^{3}MLCT states in **Re-2** - **Re-4** lie at approximately 3.0 and 1.7 eV, respectively. These energies are used in the diagram shown in Figure 11b.

Finally, consider the excited-state diagram for the CH_3CN substituted complexes **ReACN-2** and **ReACN-3** (Figure 11c). Since it is anticipated that substitution of Cl for CH_3CN will not affect the energies of the π,π^* states for the OAE π-system, these states are positioned the same in **ReACN-2** and **ReACN-3** as in **Re-2**−**Re-4**. However, the ^{1}MLCT and ^{3}MLCT states of (bpy)Re(CO)$_3$(NCCH$_3$)$^+$ are approximately 0.35 eV higher in energy relative to the same states in (bpy)Re(CO)$_3$Cl. On the basis of this energy difference, it is expected that the ^{1}MLCT and ^{3}MLCT states will be increased a similar amount in **ReACN-2** and **ReACN-3** relative to the energies of the states in **Re-2**−**Re-4**. This places the states at 2.05 and 3.3 eV, respectively.

This analysis raises several important issues regarding the lowest excited states in the metal−OAEs. First, it is evident that in all of the metal−organic oligomers the $^3\pi,\pi^*_c$ and ^{3}MLCT states are in close energetic proximity. This close proximity makes it possible that both states will contribute to the observed photophysics. Second, it is also clear that the state ordering is switched in the two series: for the Cl-substituted complexes, **Re-2**−**Re-4**, ^{3}MLCT is lowest in energy, while in the CH_3CN-substituted complexes, **ReACN-2** and **ReACN-3**, $^3\pi,\pi^*_c$ is lowest. As discussed below, this switch in state ordering is believed to be responsible for the significant difference in excited-state dynamics in the two families of complexes.

Photophysics of the Metal−Organic Oligomers. The variable temperature PL spectra of **Re-2**−**Re-4**, **ReACN-2**, and **ReACN-3** are qualitatively similar (Figures 4 and 8). Specifically, at $T > 200$ K, the PL is dominated by a structured band with $\lambda_{max} \approx 650$ nm, while at lower temperatures a second broad band appears at higher energy. The structured 650 nm emission band is assigned to phosphorescence from the triplet excited state of the "core" chromophore ($^3\pi,\pi^*_c$) on the basis of the following facts: (1) The emission energy corresponds exactly to the energy that is predicted for this state (vide supra). (2) The energy of the structured emission does not change significantly when the solvent glass point is reached. (A blue-shift is expected if the emission arises from an MLCT state due to the rigidochromic effect.[49])

The origin of the broad emission band that appears on the blue edge of the $^3\pi,\pi^*_c$ phosphorescence as the temperature is lowered is less certain. An important consideration in the assignment of this band is that its apparent λ_{max} decreases with

(82) Manas, E. S.; Chen, L. X. *Chem. Phys. Lett.* **2000**, *331*, 299−307.

(83) The large error is due to the fact that the electrochemical potentials for the two systems have been determined in different solvent media and with different working electrodes.

temperature. As noted above, a blue-shift with decreasing temperature is characteristic for charge-transfer emission,[49] and on the basis of this point we suggest that the broad band emanates from the ^{3}MLCT excited state.

The PL spectra of **Re-2**−**Re-4**, **ReACN-2** and **ReACN-3** indicate that both low-lying excited states, $^3\pi,\pi^*_c$ and ^{3}MLCT, are populated to a significant extent at times >1 ns following excitation. The dual emission implies that these two excited states are in equilibrium.[67,68] Further information concerning this equilibrium comes from consideration of the TA and emission decay kinetics (Table 2).

For the Cl-substituted complexes (**Re-2**−**Re-4**) there is good agreement between the TA decay lifetime and the lifetime of the long-lived PL decay component. In addition, the excited-state decay lifetimes are consistent with those expected for a ^{3}MLCT state in a (diimine)Re^I(CO)$_3$Cl complex.[50] Taken together, these facts are supported by the excited-state model in Figure 11b. Thus, for **Re-2**−**Re-4**, the lowest excited state is ^{3}MLCT. However, because $^3\pi,\pi^*_c$ is only slightly higher in energy, it is populated via the equilibrium (step 6, Figure 11b). Since ^{3}MLCT is lower in energy and has a relatively large nonradiative decay rate constant (step 9, Figure 11b, $k_9 \approx 10^6-10^7$ s^{-1}),[50] decay via this state is the main deactivation mode, and the rate of this process controls the overall lifetime of the excited-state population.[67−73]

Despite the fact that in **Re-2**−**Re-4** ^{3}MLCT is lowest in energy and is responsible for the relatively rapid decay of the excited state, we believe that the TA spectra of **Re-2**−**Re-4** are dominated by the $^3\pi,\pi^*_c$ state. This assignment is based primarily on the fact that the difference spectra of the excited complexes are nearly indistinguishable from those of **ReACN-2** and **ReACN-3**, and in the latter complexes there is ample data to support assignment of the long-lived transient absorption to the $^3\pi,\pi^*_c$ state (vide infra). It is likely that the difference molar absorptivity ($\Delta\epsilon$) for the $^3\pi,\pi$ state is very large, and this also may account for the fact that this state dominates the TA spectra, that is, the absorption of the ^{3}MLCT state is obscured by the stronger absorbance of $^3\pi,\pi$. (It is also possible that the difference spectra of the $^3\pi,\pi^*_c$ and MLCT states are similar.)

The striking feature for the CH_3CN substituted complexes **ReACN-2** and **ReACN-3** is that their TA decay lifetimes are considerably longer than those for **Re-2**−**Re-4** (Table 2). In addition, the TA decay lifetimes for **ReACN-2** and **ReACN-3** are several orders of magnitude longer than their PL decay lifetimes. These data are consistent with the excited-state model presented in Figure 11c. Thus, for the CH_3CN complexes, the $^3\pi,\pi^*_c$ state is lowest in energy, with ^{3}MLCT lying somewhat higher in energy. Because of this state ordering the equilibrium favors the $^3\pi,\pi^*_c$ state, and at long times after excitation the excited-state population resides mainly in this state. Consequently, the TA difference spectra of these complexes is clearly due to the $^3\pi,\pi^*_c$ state. In addition, the EPR signature of this state can be observed at low temperature by TREPR (Figure 10).

Although the transient absorption lifetimes of **ReACN-2** and **ReACN-3** are considerably longer than typical for a ^{3}MLCT state, they are considerably shorter than expected for organic triplets. For example, the triplet lifetimes of the oligomers **1**−**4** are >100 μs (Table 1). The "reduced" lifetimes of the $^3\pi,\pi^*_c$ states in **ReACN-2** and **ReACN-3** likely arise because the dominant excited-state decay channel is via thermally activated population of the ^{3}MLCT state (i.e., step 6, followed by step 9 in Figure 11c). It is also possible that spin−orbit coupling induced by the rhenium ion may increase the rate of direct triplet relaxation via intersystem crossing (i.e., step 10 in Figure 11c).

Finally we consider the origin of the fast emission decay components ($\tau \approx 1$ ns) and the large amplitude decay observed by ps transient absorption ($\tau \approx 700$ ps). While it is tempting to assign these processes to energy transfer and intersystem crossing within the OAE chain, we believe that the decays correspond to establishment of the equilibrium between the ^{3}MLCT and $^3\pi,\pi^*_c$ excited states.[84] Thus, we suggest that for all of the complexes excitation populates the $^1\pi,\pi^*$ manifold (steps 1 and 2, Figure 11, b and c). Subsequently, ultrafast energy transfer and intersystem crossing ensues to afford a nonequilibrium distribution of the ^{3}MLCT and $^3\pi,\pi^*_c$ states (i.e., paths 3, 4, and 5 in Figure 11, b and c occur with $\tau < 20$ ps). On the basis of experimental evidence that indicates that in diimine transition-metal complexes the ^{3}MLCT manifold is populated very rapidly following excitation,[85] we favor an interpretation where the dominant ultrafast relaxation in the metal−organic complexes affords mainly ^{3}MLCT (i.e., $k_5 > k_4$, where subscripts refer to processes in Figure 11, b and c). If this model is correct, then the fast PL and TA decay components observed for **Re-2**−**Re-4** correspond to the rate of ^{3}MLCT → $^3\pi,\pi^*_c$ energy transfer. For **ReACN-2** and **ReACN-3** virtually all of the PL decays in less than 1 ns. This is consistent with the fact that the $^3\pi,\pi^*$ state is lower in energy compared to ^{3}MLCT in these complexes, and because of this state ordering the lifetime of ^{3}MLCT is expected to be very short.

Photophysics of Re-1. The previous discussion centered on the longer metal−OAEs, which all share the common core chromophore. The situation for the shortest OAE complex (**Re-1**) is different because in this system the energy of the $^3\pi,\pi^*$ state is higher due to the shorter π-conjugated segment. On the basis of the blue-shift of the lowest-energy absorption band (∼35 nm relative to the maxima of **Re-2**−**Re-4**) we estimate that in **Re-1** the $^3\pi,\pi^*$ state is at ∼2.1 eV. Thus, it is clear that in **Re-1** at ambient temperature ^{3}MLCT is the lowest excited state, since based on the electrochemistry the energy of ^{3}MLCT is similar in all of the metal−OAE complexes (i.e., the reduction potential for all of the complexes is ∼−0.9 V). The MLCT assignment is supported by the broad emission band with $E_{max} \approx 1.8$ eV (see inset, Figure 4a) and by the lifetime (20 ns), which is comparable to that of the parent complex. Given the MLCT assignment for the emission, then it follows that the TA difference spectrum of **Re-1** (Figure 5a) can be assigned to the MLCT state. Although there are clear differences in the TA spectra of **Re-1** and the longer oligomers, it is interesting to note that the excited state difference spectra exhibit qualitatively similar features, despite the fact that they arise from states of different orbital character (i.e., dπ,π^* and π,π^*).

The PL of **Re-1** develops a well-defined vibronic structure, blue-shifts, and increases significantly in intensity at low temperatures (Figure 4a). These features are characteristic of MLCT emission,[49] making it tempting to assign the low-temperature PL from **Re-1** to the ^{3}MLCT state. However, it is important to recognize that due to the increased energy of the

(84) It is unclear why the amplitude of the fast emission decay component is so large relative to that of the slow component in **Re-2**−**Re-4**. It is possible that some of the fast decay component arises from the very short-lived $^1\pi,\pi^*$ manifold (i.e., fluorescence). In this case, because of the large radiative decay rate of the $^1\pi,\pi^*$ state, the amplitude of the fast component would be expected to be large compared to that of the MLCT state, which has a considerably lower radiative decay rate. In support of this hypothesis it was observed that the amplitude of the fast component is larger when the emission decay is obtained on the blue edge of the emission band.

(85) Damrauer, N. H.; Cerullo, G.; Yeh, A.; Boussie, T. R.; Shank, C. V.; McCusker, J. K. *Science* **1997**, *275*, 54−57.

^{3}MLCT state in the low-temperature glass, under these conditions the ^{3}MLCT and $^3\pi,\pi^*$ states are close in energy. It is therefore possible that the PL observed at low temperature arises from both excited states, as is the case for the longer metal−OAEs.

Conclusions

This report describes the first comprehensive examination of the photophysics of a series of well-defined π-conjugated oligomers that contain the d^6 (diimine)$Re^I(CO)_3Cl$ (MLCT) chromophore. These compounds feature a rich and complicated array of excited states that are based on both the π-conjugated oligomer system and the MLCT chromophore. The oligomers absorb strongly throughout the near-UV and into the visible region and the absorption spectra of the metal−oligomers are dominated by the π,π^* transitions. Little direct evidence for Re → bpy-oligomer MLCT absorption is observed. Although the unmetalated oligomers are strongly fluorescent, the fluorescence from the metalated oligomers is largely quenched. The fluorescence is replaced by a weak, red photoluminescence that is believed to emanate primarily from the $^3\pi,\pi^*$ manifold of the OAE π-system. Transient absorption and TREPR spectroscopy provides additional evidence that the long-lived excited state in the metal−oligomers is $^3\pi,\pi^*$ in nature.

Due to the involvement of the OAE-based $^3\pi,\pi^*$ states in the photophysics of the metal−oligomers, it is not possible to clearly assess the influence of the π-conjugated electronic system on the properties of the Re → bpy-oligomer MLCT excited state. For example, in previous work it has been demonstrated that increased conjugation in the diimine "acceptor" ligand decreases the nonradiative decay rate of an MLCT state due to decreased electron-vibrational coupling.[86,87] Although the excited-state lifetimes of **Re-2**−**Re-4** are enhanced by almost a factor of 10 compared to the parent complex (bpy)$Re(CO)_3Cl$, due to the close energetic proximity of the OAE-based $^3\pi,\pi^*_c$ state it is unclear whether the enhanced lifetimes can be attributed solely to a decreased nonradiative decay rate for the MLCT state or whether there is some (configuration) interaction between the states that influences the observed nonradiative decay rates. Such conclusions must await further studies that will explore metal−oligomer systems that are designed specifically to raise the energy of the $^3\pi,\pi^*$ states relative to the MLCT manifold.

Acknowledgment. This work was carried out with the support of the National Science Foundation under Grant CHE-9901862 (K.S.S., K.A.W., and K.D.L.). Work at the University of Massachusetts, Northwestern University, and Argonne National Laboratory was supported by the Division of Chemical Sciences, Office of Basic Energy Sciences of the U.S. Department of Energy under Grants DE-FG02-84ER-13242 (H.v.W.) and DE-FG02-99ER-14999 (M.R.W.) and Contract W-31-109-Eng-38 (D.G.).

Supporting Information Available: A figure illustrating Sandros Plots for triplet quenching of OAEs **1**, **3**, and **4**. This material is available free of charge via the Internet at http://pubs.acs.org. See any current masthead page for ordering information and Web access instructions.

JA015813H

(86) Strouse, G. F.; Schoonover, J. R.; Duesing, R.; Boyde, S.; Jones, W. E., Jr.; Meyer, T. J. *Inorg. Chem.* **1995**, *34*, 473−487.

(87) Grosshenny, V.; Harriman, A.; Romero, F. M.; Ziessel, R. *J. Phys. Chem.* **1996**, *100*, 17472−17484.

(88) Perkins, T. A.; Humer, W.; Netzel, T. L.; Schanze, K. S. *J. Phys. Chem.* **1990**, *94*, 2229−2232.

(89) Paolucci, F.; Marcaccio, M.; Paradisi, C.; Roffia, S.; Bignozzi, C. A.; Amatore, C. *J. Phys. Chem. B* **1998**, *102*, 4759−4769.